Radiotherapy and Oncology 163 (2021) 143–149

Contents lists available at ScienceDirect

Radiotherapy and Oncology

journal homepage: www.thegreenjournal.com

Original Article

Study of relationship between dose, LET and the risk of brain necrosis after proton therapy for skull base tumors

Magdalena Garbacz [a,*], Francesco Giuseppe Cordoni [b,c], Marco Durante [d,e], Jan Gajewski [a], Kamil Kisielewicz [f], Nils Krah [g,l], Renata Kopeć [a], Paweł Olko [a], Vincenzo Patera [h,i], Ilaria Rinaldi [j], Marzena Rydygier [a], Angelo Schiavi [i], Emanuele Scifoni [c], Tomasz Skóra [f], Francesco Tommasino [c,k], Antoni Rucinski [a]

[a] Institute of Nuclear Physics Polish Academy of Sciences, 31342 Krakow, Poland; [b] University of Verona, Department of Computer Science, Verona, Italy; [c] Trento Institute for Fundamental Physics and Applications, TIFPA-INFN, Trento, Italy; [d] GSI Helmholtzzentrum fur Schwerionenforschung, Darmstadt, Germany; [e] The Technical University of Darmstadt, Germany; [f] National Oncology Institute, National Research Institute, Krakow Branch, Krakow, Poland; [g] University of Lyon, CREATIS, CNRS UMR5220, Inserm U1044, INSA-Lyon, Université Lyon 1, Centre Léon Bérard, France; [h] INFN - Section of Rome, Italy; [i] Department of Basic and Applied Sciences for Engineering, Sapienza University of Rome, Italy; [j] Department of Radiation Oncology (Maastro), GROW School for Oncology, Maastricht University Medical Centre+, Maastricht, The Netherlands; [k] Department of Physics, University of Trento, Trento, Italy; [l] University of Lyon, Université Claude Bernard Lyon 1, CNRS/IN2P3, IP2I Lyon, UMR 5822, Villeurbanne, France

ARTICLE INFO

Article history:
Received 15 January 2021
Received in revised form 27 July 2021
Accepted 21 August 2021
Available online 27 August 2021

Keywords:
Brain necrosis
Linear energy transfer
Monte Carlo
Proton therapy
Variable RBE

ABSTRACT

Purpose: We investigated the relationship between RBE-weighted dose (DRBE) calculated with constant (cRBE) and variable RBE (vRBE), dose-averaged linear energy transfer (LETd) and the risk of radiographic changes in skull base patients treated with protons.
Methods: Clinical treatment plans of 45 patients were recalculated with Monte Carlo tool FRED. Radiographic changes (i.e. edema and/or necrosis) were identified by MRI. Dosimetric parameters for cRBE and vRBE were computed. Biological margin extension and voxel-based analysis were employed looking for association of DRBE(vRBE) and LETd with brain edema and/or necrosis.
Results: When using vRBE, Dmax in the brain was above the highest dose limits for 38% of patients, while such limit was never exceeded assuming cRBE. Similar values of Dmax were observed in necrotic regions, brain and temporal lobes. Most of the brain necrosis was in proximity to the PTV. The voxel-based analysis did not show evidence of an association with high LETd values.
Conclusions: When looking at standard dosimetric parameters, the higher dose associated with vRBE seems to be responsible for an enhanced risk of radiographic changes. However, as revealed by a voxel-based analysis, the large inter-patient variability hinders the identification of a clear effect for high LETd.

Skull base cancers are a challenging localization for radiotherapy because irradiated tumors are often in proximity of healthy organs, which might be exposed to high doses. The normal tissue long term response to radiation remains a key challenge in radiation therapy with existing and emerging modalities [1]. Nowadays, the dose delivered to the critical organs might be reduced by replacing the conventional photon radiation with accelerated ions, e.g. protons [2], and by replacing for the latter passive scattering with pencil beam scanning (PBS) delivery techniques [3].

Protons, as they penetrate the medium, slow down and give origin to the so-called Bragg peak, with the ionisation density increasing at the end of their path and quantified by the linear energy transfer (LET) [4]. This is responsible for enhanced biological damage [5] and increased relative biological effectiveness (RBE, i.e. the ratio of photon to proton dose that are needed to obtain the same biological effect), particularly near the Bragg peak region. This RBE, which experimental evidence indicates to be higher than the clinically applied RBE = 1.1 [6–8], may be an advantage in tumor treatment, but at the same time a challenge for surrounding healthy tissues. This is due to the range uncertainty in proton therapy (both from physical [9] and biological [10] sources) and the variability of experimental RBE values [6,11].

Recently, discussion emerged concerning the possible enhanced risk of brain necrosis [12] when high doses are associated with high LET but results so far were not conclusive [13–15]. Brain injury might be diagnosed by observing symptoms like weakness, dizziness, headache or can be asymptomatic [16]. Changes in the brain structure may occur after radiation therapy at different times

* Corresponding author at: Institute of Nuclear Physics Polish Academy of Sciences, 31342 Krakow, Poland.
E-mail address: magdalena.garbacz@ifj.edu.pl (M. Garbacz).

https://doi.org/10.1016/j.radonc.2021.08.015
0167-8140/

and with different grades, and are typically diagnosed as a contrast enhancement in the brain lesion using magnetic resonance imaging (MRI) [14]. Changes in brain structure can also be caused by many other factors that are not related to radiotherapy such as: age, former surgeries, genetic vulnerability, vascular conditions and other accompanying diseases [17]. Still, for radiotherapy patients the high dose delivered to organs at risk (OARs) is considered as a key factor initiating the development of necrosis [18].

In this study we investigated the association of dose-averaged LET (LET_d) and variable RBE (vRBE) with radiographic brain changes (edema and/or necrosis). Based on a cohort of 45 patients with skull base tumors treated with protons, an extensive analysis was performed, involving both standard dosimetric parameters and more advanced voxel-based methods.

Methods

Patients database description

Data were collected from the institutional anonymised clinical database of 45 patients with skull base tumours from 95 patients in total (see Table S1 in Supplementary material). Computed tomography (CT) images (Siemens Somatom Definition AS) were acquired for each patient and structure contouring was performed. Patients involved in the study underwent intensity-modulated proton therapy (IMPT) between November 2016 and September 2018 at Cyclotron Centre Bronowice in Krakow (Poland). 28 patients had diagnosed chordoma (CH) and 17 patients had chondrosarcoma (CHS). We excluded patients who underwent replanning, pediatric cases and treatment plans optimized with a single field uniform dose (SFUD) method. All patients signed informed consent, allowing the use of treatment data for research purposes and statistical analysis.

Treatment planning and patients follow up

The patients were treated with prescription doses in the range 70.0–74.0 Gy(RBE) (see recommendation in Stacchiotti et al. [19] and NCCN Guidelines [20]) with 2.0 Gy(RBE) per fraction planned with RBE = 1.1. The details on the dose prescription are provided in Table 1. The dose was prescribed to the technical planning target volume (PTV) (constructed manually for every field), which is an extended PTV structure, including 3.5% calibration curve uncertainty plus 1 mm on distal border calculated for clinical target volume (CTV). For the calculated plan, robust evaluation for CTV and OARs was performed (but not included in this analysis). The treatment schedule was carried out in 1 or 2–3 stages, with a change in irradiated volume. Treatment planning was performed with the treatment planning system (TPS) Eclipse 13.6. The plans consisted of 2–6 irradiation fields (the median was 4 fields). All the plans were optimized using Proton Convolution Superposition v13.6.23 algorithm and dose constraints proposed by EPTN [21].

The first post-treatment control MRI scans were taken about 3 months after the end of the therapy, and were repeated at least once every 6 months, in case the patient did not show any symptom of brain injury. MRI was performed using a 1.5 T Avanto system (Siemens, Germany) examining the area of interest using a dedicated head and neck coil. T1 weighted images with and without fat saturation were acquired in coronal, sagittal and transverse planes and T2 weighted images in transversal plane were obtained before the intravenous contrast injection (0.1 mmol/kg body weight of Gadovist (gadobutrol) followed by the saline bolus). After contrast administration T1 sequences were repeated with the same parameters as before. The slice thickness in these sequences varied from 2.5 to 5 mm depending on the sequence and plane orientation.

Brain radiographic changes were defined as contrast-enhancing brain lesions (CEBL), which were delineated by a medical doctor using the first MRI images where changes have been detected. Based on MRI, such patients were then diagnosed with symptomatic or non-symptomatic brain changes, which according to Late Effects Normal Tissue Task Force subjective, objective, management and analytic (LENT-SOMA) were divided into edema (necrosis grade 1, mostly visible on T2/FLAIR acquisitions [22,23]) or/and necrosis grade from 2 to 3 structure (identified on T1 acquisitions with contrast). Table 1 summarizes the characteristics of patients showing CEBL.

Deposited D_{RBE} and dose constraints for brain necrosis

Dose recalculation was performed with a $1.5 \times 1.5 \times 1.5$ mm^3 voxel grid, using the Monte Carlo tool FRED (Fast paRticle thErapy Dose evaluator) [24], which outputs three dimensional (3D) maps of deposited physical dose, D_{RBE} and LET_d. The CT calibration curve for FRED simulations was obtained from stoichiometric calibration (as presented in Schneider et al. [25]) and the values from the calibration curve, i.e. the relative stopping power and the Hounsfield Units (HU) were related to the elemental composition of the materials. Fig. 1 shows MRI, D_{RBE} and LET_d-volume histogram for examplonary patients. When the plan included more than one stage, an average LET_d was computed, by calculating for each voxel an average LET value weighted by the dose delivered in each stage. For each patient, we analysed deposited D_{RBE} calculated with cRBE (RBE = 1.1) and vRBE parametric model by McNamara [19], assuming α/β = 4 Gy in PTV (based on [26,27]) and α/β = 2 Gy for brain, left and right temporal lobe (LTL and RTL, respectively). The choice of α/β ratio was based on the tumor type and data presented in van Leeuwen et al. [27].

Table 1
Patient information with diagnosed CEBL. Abbreviations: CH - chorodma, CHS - chondrosarcoma, R-recurrence, P - primary, Dp - prescribed dose, LTL - left temporal lobe, RTL - right temporal lobe, BS - brain stem, LH - left hippocampus, RH - right hippocampus, B - brain.

Patient no	Diagnosis	Characteristic	Total dose (per stage) [Gy(RBE)]	PTV volume [cm^3]	Necrosis/ edema location	Grade of necrosis	Symptoms	Necrosis dynamic	Necrosis/edema volume [cm^3]
57	CHS	primary	70 (54 + 16)	165.5, 138.9	B	1	no	stable	none/0.22
63	CH	recurrence	74	99.8	LTL, LH, BS	2	yes	regress	5.96/48.29
81	CHS	primary	70 (54 + 16)	105.4, 67.6	RTL	1	no	stable	1.37/7.46
82	CH	primary	70	64.3	LTL	1	no	progress	0.25/1.25
89	CHS	primary	70 (54 + 16)	85.7, 65.3	LTL, LH	1	no	progress	4.22/29.61
90	CH	primary	74	95.7	RTL, LTL, RH	1	no	progress	0.3/2.89
91	CHS	recurrence	74 (54 + 20)	87.3, 30.7	LTL, LH	2	yes	progress	0.09/none
92	CHS	recurrence	70 (54 + 16)	147.3, 66.9	LTL, LH	3	yes	progress	0.36/6.55
95	CHS	primary	74 (54 + 16 + 4)	123.0, 83.8, 29.3	RTL, RH	2	yes	progress	none/35.1

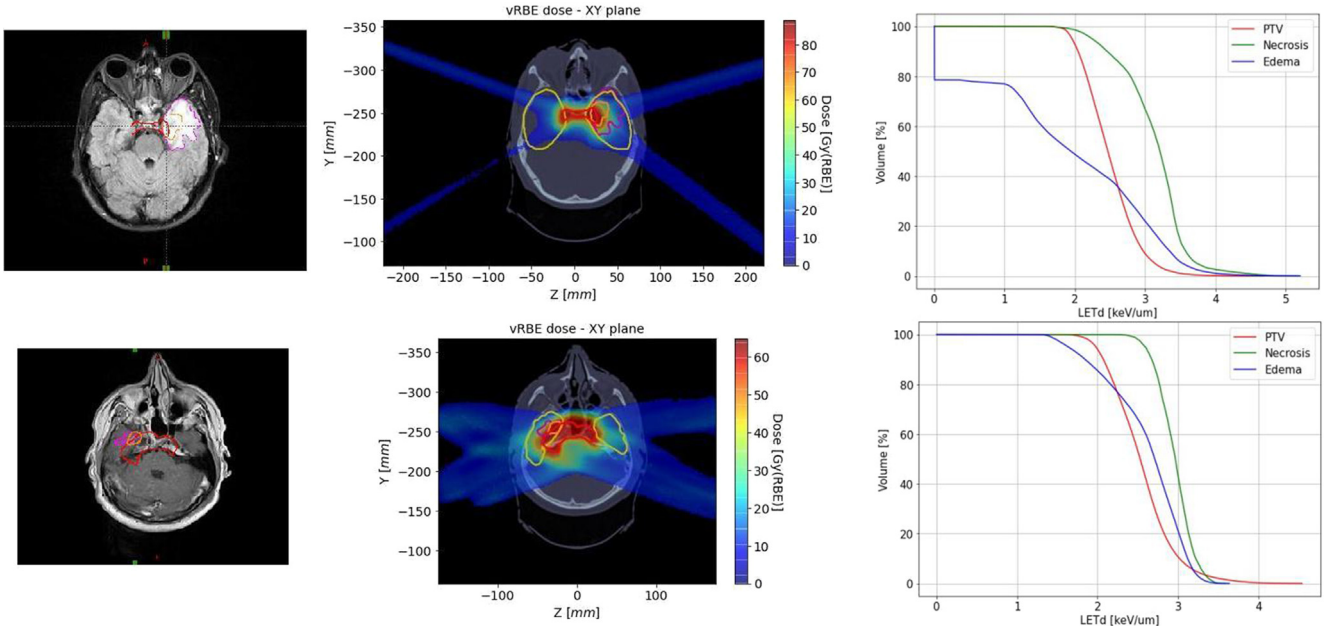

Fig. 1. MRI, dose distribution and LET_d-volume histogram with delineated PTV (red), temporal lobes (yellow), necrosis (orange) and edema (magenta) for Patient 63 (top row) and Patient 81 (bottom row). (For interpretation of the references to colour in this figure legend, the reader is referred to the web version of this article.)

The D_{max} from the brain and necrosis/edema regions was extracted and compared with dose constraints proposed by Marks et al. [18], which include recommendations for analysing the risk of symptomatic necrosis. The dose to the RTL and LTL were compared with dose constraints from Pehlivan et al. [28]. As a representative parameter for the dose delivered to the temporal lobes we have chosen D02 (the dose delivered to 2% of the structure volume), which typically refers to a volume of around 2 cubic centimeters (D2cc), as suggested in Pehlivan et al. [28] and in Feng et al. [29].

Biological margin extension and brain necrosis

We defined biological margin extension as the difference between two radiuses:

$$R_{ext} = R_{vRBE} - R_{cRBE},$$

where: R_{vRBE} - radius of sphere of V95 volume (i.e. volume covered with at least 95% of prescribed dose (D_p)) computed with vRBE, R_{cRBE} - radius of sphere of V95 volume computed with constant RBE. Further details on this method are out of the scope of this study. For our patient cohort, dedicated analysis with vRBE indicated a mean biological margin extension of 0.45 ± 0.11 cm. We therefore prepared an extended PTV volume that was defined as an isotropic extension of PTV by a 5 mm margin (which corresponds to 4.5 mm margin extension rounded to the 1 mm accuracy allowed by the TPS) in order to identify the volume associated with high D_{RBE} when the vRBE model is adopted. For each patient with diagnosed CEBL we then searched for overlap between contoured brain changes and PTV or PTV + 5 mm volumes, which we expected to indicate an association between biological margin extension and CEBL.

Voxel-based analysis

In order to investigate the association between LET_d and the risk of necrosis/edema, a voxel-based analysis was performed, in line with what was recently proposed by Niemierko et al. [13]. Specifically, for each patient the necrotic voxels were identified, and a dose-matched sample was obtained by sampling at random without replacement from the population of non-necrotic voxels (dose-matching voxels were extracted by assuming a ±0.1 Gy physical dose threshold for the selection window). The comparison between necrotic and non-necrotic voxels was then performed by looking at the distribution of LET_d and of $Dose(1 + 0.05LET_d)$, the latter being a surrogate for the LET_d-dependent biological dose [30]. The same procedure was applied for the analysis of edema regions.

Statistical analysis

For the comparison of dose in RTL and LTL we used Wilson score method [31] to assign a confidence interval to the probability of observing necrosis and/or edema when the dose limit of 77.7 Gy (RBE) (corresponding to 105% of the D_p of 74 Gy(RBE) for chordomas) [28] is exceeded.

The I-squared (I^2) statistics is adopted as heterogeneity metrics for the analysis of necrosis and edema patients. Box-plots are employed to summarize the voxel distributions resulting from the matched-paired analysis.

Results

The D02 parameter was calculated for LTL (left column) and RTL (right column) together with D_{max} for necrosis and/or edema, when present (Figs. 2 and S11 in Supplementary materials). The D_{max} observed in necrosis/edema shows values close to the D02 parameter in LTL and RTL. The dose calculated with vRBE, in contrast to the dose calculated with cRBE, exceeded dose limits for more than half of the patients. We observed that necrosis appeared when doses computed with vRBE were higher than 77.7 Gy(RBE) both, for LTL and RTL. The probability of radiographic changes in LTL, when exceeding dose limit, was 0.15 [95%CI: 0.07,0.29], while for RTL it was 0.22 [95%CI: 0.12,0.38].

Fig. S10 in Supplementary shows D_{max} values in the brain and necrosis and/or edema structure from dose distributions calculated with cRBE and vRBE. We highlighted dose limits equal to 60, 72 and 90 Gy(RBE) corresponding to 3%, 5% and 10% risk of necrosis [18], respectively. With vRBE, D_{max} deposited in the brain was

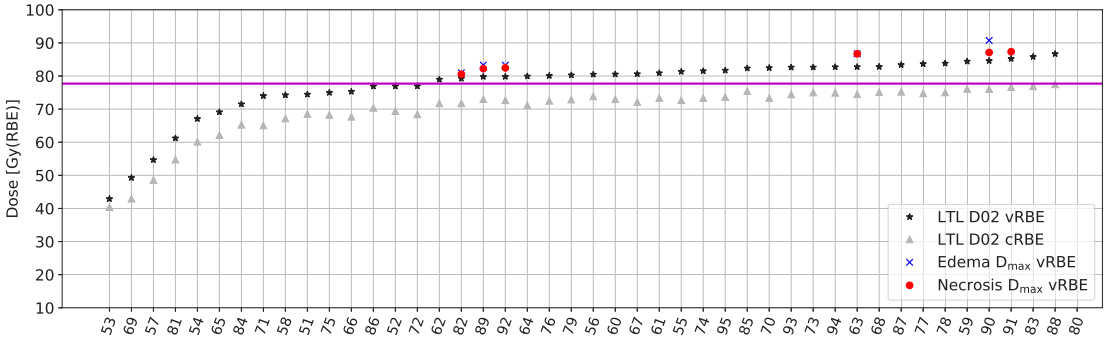

Fig. 2. D02 for left temporal lobe calculated with constant and variable RBE and D_{max} in necrosis/edema calculated with vRBE. Solid magenta line indicates the dose constraint at 77.7 Gy(RBE).

above the highest dose limits for 38% of patients, while such limit was never exceeded assuming cRBE. When necrosis or edema are identified, the values of D_{max} in such regions were similar to those in the brain tissue.

Concerning the biological margin extension analysis, the volume of necrosis and edema, which intersects with the PTV and PTV + 5 mm were compared (Fig. 3). Results show that the fraction of the necrosis volume which lies inside the PTV + 5 mm was on average 23% larger compared to the fraction of the necrosis volume associated with the primary PTV. Similarly, the fraction of edema volume increased on average by 13% for the expanded PTV compared to the primary one. Furthermore, we noticed that, for 4 of the 7 patients showing necrosis, 100% of the necrosis volume was covered by the extended PTV. For the rest of the patients the extended PTV covered at least 55% of the necrotic region.

The results of the voxel-based analysis are summarized in Figs. 4 and 5 for necrosis and edema, respectively. Firstly, Fig. 4 indicates a large variability in the size of the necrosis (0.09–48.29 cm^3). When looking at the average LET_d in necrotic and non-necrotic regions, the average tendency was observed of a slightly enhanced LET_d for the first (3.0 keV/μm vs 2.8 keV/μm). However, for one patient a higher LET_d was associated with the non-necrotic voxels, and for two of them the average LET_d was virtually identical. Despite average values, remarkable differences in LET_d distributions were observed among necrotic and non-necrotic regions, as suggested by the box plots. When looking at the single patients, the fluctuations described above were observed, which finally resulted in an average difference of 0.22 keV/μm. This indicates a weak increase in average LET_d for the necrotic voxels. When looking at the edema data in Fig. 5, an even lower difference was observed compared to necrosis. The I^2 statistics indicated substantial (I^2 = 57% for necrosis analysis) to strong (I^2 = 89% for edema analysis) heterogeneity among patients. The analysis performed for Dose(1 + 0.05LET_d) basically mirrors the behaviour observed for LET_d. The results are reported in Supplementary materials.

Discussion

In the present paper we analyzed D_{RBE} computed with cRBE and vRBE as well as LET_d distributions for skull base patients. The risk of edema and/or necrosis was investigated for individual patients receiving IMPT.

From the analysis of D_{RBE} deposited in the brain and computed with vRBE we found that almost all patients had at least 5% risk of developing necrosis according to the risk level established in Marks et al. [18]. The D_{max} values (Fig. S10) in necrosis/edema had similar values to the D_{max} in the whole brain structure, which can indicate that necrosis appeared in the location of the highest dose computed with vRBE and was associated with regions of the highest dose.

We compared our findings in terms of the deposited dose in structures where necroses begin to appear, with dose limits for the temporal lobe using DVH parameter D02 of 77.7 Gy(RBE). Our study shows that necrosis or edema appeared in patients with D02 < 80 Gy(RBE) in temporal lobes, computed with vRBE, which is similar to the results from Pehlivan et al. [28].

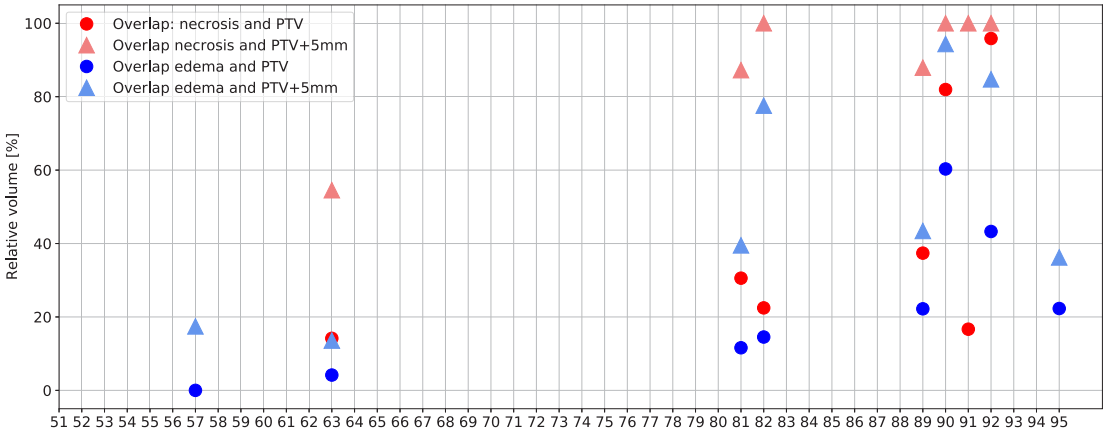

Fig. 3. Relative volumes of necrosis and edema overlapped with PTV and extended PTV regions.

Patient no	Mean LET (keV/μm)		Mean Difference (keV/μm)	Nr of necrotic voxels
	Necrotic	Non-necrotic		
92	2.54	2.66	-0.12±0.02	699
89	2.81	2.80	0.01±0.01	7602
90	2.99	2.93	0.07±0.03	554
82	2.97	2.79	0.18±0.04	494
81	2.94	2.72	0.22±0.02	2506
63	3.13	2.68	0.45±0.02	5236
91	3.58	2.82	0.76±0.09	102
Mean	2.99	2.77	0.22±0.03	2456.14

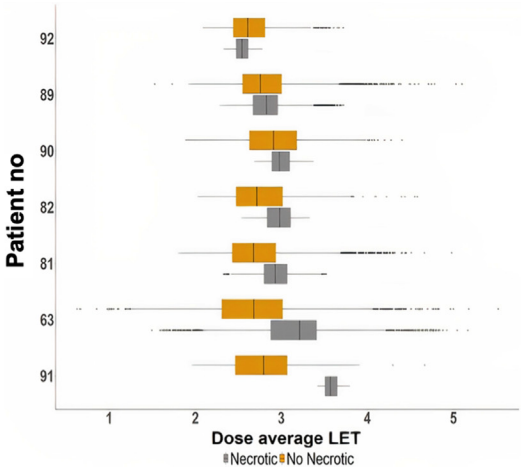

Fig. 4. Summary of LET analysis for dose-matched voxels. The left table shows average LET for necrotic and dose-matching non-necrotic regions for each patient, together with their difference; the last table line summarizes the statistics over all tested patients. The right plot shows for each patient the corresponding boxplots of LET for necrotic (grey) and not necrotic (orange) regions. Outliers are identified as individual data points outside the boxplots. The I^2 = 57% is reported as a measure of data heterogeneity. (For interpretation of the references to colour in this figure legend, the reader is referred to the web version of this article.)

Patient no	Mean LET (keV/μm)		Mean Difference (keV/μm)	Nr of necrotic voxels
	Edema	Non-edema		
57	1.51	2.76	-1.25±0.07	413
95	2.00	2.3	-0.30±0.01	63310
90	2.89	2.97	-0.07±0.01	5279
92	2.72	2.75	-0.03±0.01	11862
81	2.56	2.58	-0.02±0.01	13538
82	2.95	2.90	0.05±0.02	2278
89	2.50	2.41	0.09±0.01	52846
63	2.39	2.19	0.2±0.04	42542
Mean	2.44	2.61	-0.17±0.02	24008.5

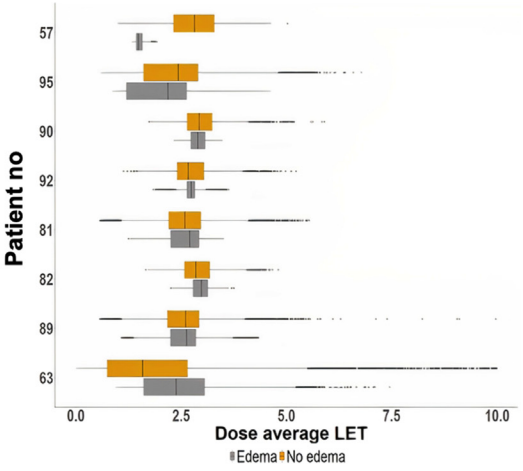

Fig. 5. Same as in Fig. 4, but the edema regions are analyzed here. The I^2 = 89.2% is reported as a measure of data heterogeneity.

Overall, the voxel-based analysis indicates a minor influence of LET_d on the risk of developing edema/necrosis. For most of the patients, the matched-pair comparison revealed the tendency of similar average LET_d values in normal brain voxels compared to edema/necrotic ones (Figs. 4 and 5). In some cases, a higher average LET_d was associated with normal tissues compared to necrotic ones. This is similar to what was observed by Niemierko [13], and indicates a large inter-patient variability that might hide correlation. Moreover, despite the average similarity in average values, we observed remarkable differences in LET_d distributions for normal tissues compared to the necrosis. This also emerges when looking at the box-plots in Figs. 4 and 5, indicating that a narrow LET_d distribution was usually associated with necrotic voxels, while much broader ones were observed for normal tissues (see Supplementary Figs. 14–15). Consequently, the highest LET_d values were usually observed in normal tissue, which at the same time also included voxels with low LET_d. This might indicate that single-voxel LET_d was not sufficient for prediction of necrosis and that further aspects, as for instance the spatial distribution of LET_d in brain structures, might have played a role. Further study, based on a larger patient cohort is needed to further investigate this hypothesis.

The uncertainties in proton beam range might cause the delivery of higher dose in the regions outside the PTV. Beside the well-known physical uncertainty sources, such as physical modeling, CT calibration, patient movements, the vRBE contributes as an additional biological source, which includes the uncertainty of α/β ratio as discussed in Underwood et al. [32] and Paganetti [6]. Our analysis indicates that in all patients showing necrosis of grade 2 and 3, the lesion was at least partially localized in the PTV + 5 mm. At the same time, a recent study on IMPT optimization techniques showed a similar dose increase resulting from physical uncertainties compared to that related to vRBE [33]. We conclude that, while physical uncertainties must be also taken into account, the analysis of extended proton beam range might potentially predict regions that are more likely to develop necrosis of higher grade, but not necessarily edema.

Recently, several publications were dedicated to the analysis of brain injury risk in patients treated with protons, presenting conflicting evidence on the predictive power of D_{RBE}, LET_d or LET_t for such endpoints [13–15,28,29]. Firstly, it is worth mentioning the previous work by Peeler et al. [34] who were the first to report an increased probability of MR-based brain tissue changes for pediatric patients associated with D_{RBE} and high LET_t, and the more

recent investigation by Niyazi et al. [35], who proposed instead the equivalent uniform dose as a predictor for brain necrosis risk, with a different parameterization for intracranial and extracranial tumors. The results from Niemierko et al. [13] do not provide evidence of correlation between high LET_d and necrosis regions, which is in-line with our results. The authors suggest that the influence of interpatient variability (e.g. radiosensitivity, size of necrosis, timing of MRI scans) might be too strong to allow the identification of LET_d related effects. Eulitz et al. [15] were able to develop a multivariable logistic regression model that, based on D_{RBE} and LET_t, can predict late (>6 months) brain image changes. Similarly, Bahn et al. [14] by looking at CEBL in glioma patients showed an increased RBE for high LET regions. The two latter studies also used a contoured ventricular or periventricular region as an additional covariate element, which seems to increase the predictive power. The patient cohort in the studies was larger compared to our investigation, while prescription doses were on average lower. The limited number of necrosis observed in our study, together with patient heterogeneity, hindered the development of an additional predictive model, which was not investigated.

PBS proton therapy greatly reduces dose to healthy organs compared to conventional radiotherapy [36]. Most of the previous studies on necrosis occurrence as a side effect of proton therapy were performed using beam delivery systems equipped with passive scattering [37]. PBS is expected to reduce dose before the PTV region compared to passive delivery systems. This further reduces, but not eliminates, the risk of normal tissue side effects [38].

Performing systematic study on brain tissue necrosis is challenging. Apart from uncertainties discussed above, other clinical covariates might also contribute to the bias as for instance patient comorbidities and lifestyle [39]. In this context, the setup of inter-institutional studies and standardization of methods of analysis, including the consistency in LET calculation, might be essential to identify a relationship between brain injury and D_{RBE}/LET_d effects [40]. Considering the high clinical relevance of such endpoints, in our opinion the topic deserves further investigation and the efforts appear to be justified.

Conflicts of interest

None.

Acknowledgements

This project was carried out within the Reintegration programme of the Foundation for Polish Science co-financed by the EU under the European Regional Development Fund - grant no. POIR.04.04.00-00-2475/16-00. MG acknowledges the support of InterDokMed project no. POWR.03.02.00-00-I013/16. INFN Call MoVe-IT is also acknowledged. We acknowledge Prof. Jan Swakoń from the Department of Radiation Research and Proton Radiotherapy Institute of Nuclear Physics in Krakow for valuable support and sharing knowledge on proton therapy. We acknowledge the support of NVIDIA Corporation with the donation of the GPU used for this research.

Appendix A. Supplementary data

Supplementary data to this article can be found online at https://doi.org/10.1016/j.radonc.2021.08.015.

References

[1] Emami B, Lyman J, Brown A, Cola L, Goitein M, Munzenrider JE, et al. Tolerance of normal tissue to therapeutic irradiation. Int J Radiat Oncol Biol Phys 1991;21:109–22.
[2] Langendijk JA, Boersma LJ, Rasch CRN, van Vulpen M, Reitsma JB, van der Schaaf A, et al. Clinical trial strategies to compare protons with photons. Semin Radiat Oncol 2018;28:79–87.
[3] Grosshans DR, Zhu XR, Melancon A, Allen PK, Poenisch F, Palmer M, et al. Spot scanning proton therapy for malignancies of the base of skull: treatment planning, acute toxicities, and preliminary clinical outcomes. Int J Radiat Oncol Biol Phys 2014;90:540–6.
[4] KRAFT G. Tumor therapy with heavy charged particles. Prog Part Nucl Phys 2000;45:S473–544.
[5] Mohan R, Peeler CR, Guan F, Bronk L, Cao W, Grosshans DR. Radiobiological issues in proton therapy. Acta Oncol 2017;56:1367–73.
[6] Paganetti H. Relative biological effectiveness (RBE) values for proton beam therapy. Variations as a function of biological endpoint, dose, and linear energy transfer. Phys Med Biol 2014;59:R419–72.
[7] Ödén J, DeLuca PM, Orton CG. The use of a constant RBE=1.1 for proton radiotherapy is no longer appropriate. Med Phys 2018;45:502–5.
[8] Gulliford SL, Prise KM. Relative biological effect/linear energy transfer in proton beam therapy: a primer. Clin Oncol 2019;31:809–12.
[9] Paganetti H. Range uncertainties in proton therapy and the role of Monte Carlo simulations. Phys Med Biol 2012;57:R99–R117.
[10] Carabe A, Moteabbed M, Depauw N, Schuemann J, Paganetti H. Range uncertainty in proton therapy due to variable biological effectiveness. Phys Med Biol 2012;57:1159–72.
[11] Paganetti H, Niemierko A, Ancukiewicz M, Gerweck LE, Goitein M, Loeffler JS, et al. Relative biological effectiveness (RBE) values for proton beam therapy. Int J Radiat Oncol Biol Phys 2002;53:407–21. https://doi.org/10.1016/S0360-3016(02)02754-2.
[12] Verma N, Cowperthwaite MC, Burnett MG, Markey MK. Differentiating tumor recurrence from treatment necrosis: a review of neuro-oncologic imaging strategies. Neuro Oncol 2013;15:515–34.
[13] Niemierko A, Schuemann J, Niyazi M, Giantsoudi D, Maquilan G, Shih HA, et al. Brain necrosis in adult patients after proton therapy: is there evidence for dependency on linear energy transfer? Int J Radiat Oncol Biol Phys 2021;109:109–19. https://doi.org/10.1016/j.ijrobp.2020.08.058.
[14] Bahn E, Bauer J, Harrabi S, Herfarth K, Debus J, Alber M. Late contrast enhancing brain lesions in proton-treated patients with low-grade glioma: clinical evidence for increased periventricular sensitivity and variable RBE. Int J Radiat Oncol Biol Phys 2020;107:571–8.
[15] Eulitz J, Troost EGC, Raschke F, Schulz E, Lutz B, Dutz A, et al. Predicting late magnetic resonance image changes in glioma patients after proton therapy. Acta Oncol 2019;58:1536–9.
[16] Vellayappan B, Tan CL, Yong C, Khor LK, Koh WY, Yeo TT, et al. Diagnosis and management of radiation necrosis in patients with brain metastases. Front Oncol 2018;8. https://doi.org/10.3389/fonc.2018.00395.
[17] Mao Y-P, Zhou G-Q, Liu L-Z, Guo R, Sun Y, Li L, et al. Comparison of radiological and clinical features of temporal lobe necrosis in nasopharyngeal carcinoma patients treated with 2D radiotherapy or intensity-modulated radiotherapy. Br J Cancer 2014;110:2633–9. https://doi.org/10.1038/bjc.2014.243.
[18] Marks LB, Yorke ED, Jackson A, Ten Haken RK, Constine LS, Eisbruch A, et al. Use of normal tissue complication probability models in the clinic. Int J Radiat Oncol Biol Phys 2010;76:S10–9.
[19] Stacchiotti S, Sommer J. Chordoma Global Consensus Group. Building a global consensus approach to chordoma: a position paper from the medical and patient community. Lancet Oncol 2015;16:e71–83.
[20] Susman E. New guidelines from NCCN for chordoma & giant cell bone tumors. Oncol Times 2013;35:20–1. https://doi.org/10.1097/01.cot.0000429630.77955.d4.
[21] Eekers D, Lambrecht M, De Witt Nyström P, Swinnen A, Wesseling FWR, Roelofs E, et al. EPTN consensus-based guideline for the tolerance dose per fraction of organs at risk in the brain 2018. https://doi.org/10.17195/candat.2018.01.1.
[22] Viselner G, Farina L, Lucev F, Turpini E, Lungarotti L, Bacila A, et al. Brain MR findings in patients treated with particle therapy for skull base tumors. Insights Imaging 2019;10. https://doi.org/10.1186/s13244-019-0784-9.
[23] LENT SOMA tables table of contents. Radiother Oncol 1995;35:17–60.
[24] Schiavi A, Senzacqua M, Pioli S, Mairani A, Magro G, Molinelli S, et al. Fred: a GPU-accelerated fast-Monte Carlo code for rapid treatment plan recalculation in ion beam therapy. Phys Med Biol 2017;62:7482–504.
[25] Schneider U, Pedroni E, Lomax A. The calibration of CT Hounsfield units for radiotherapy treatment planning. Phys Med Biol 1996;41:111–24.
[26] Gutierrez A, Rompokos V, Li K, Gillies C, D'Souza D, Solda F, et al. The impact of proton LET/RBE modeling and robustness analysis on base-of-skull and pediatric craniopharyngioma proton plans relative to VMAT. Acta Oncol 2019;58:1765–74.
[27] van Leeuwen CM, Oei AL, Crezee J, Bel A, Franken NAP, Stalpers LJA, et al. The alfa and beta of tumours: a review of parameters of the linear-quadratic

model, derived from clinical radiotherapy studies. Radiat Oncol 2018;13. https://doi.org/10.1186/s13014-018-1040-z.
[28] Pehlivan B, Ares C, Lomax AJ, Stadelmann O, Goitein G, Timmermann B, et al. Temporal lobe toxicity analysis after proton radiation therapy for skull base tumors. Int J Radiat Oncol Biol Phys 2012;83:1432–40.
[29] Feng M, Huang Y, Fan X, Xu P, Lang J, Wang D. Prognostic variables for temporal lobe injury after intensity modulated-radiotherapy of nasopharyngeal carcinoma. Cancer Med 2018;7:557–64.
[30] McMahon SJ, Paganetti H, Prise KM. LET-weighted doses effectively reduce biological variability in proton radiotherapy planning. Phys Med Biol 2018;63:225009.
[31] Wilson EB. Probable inference, the law of succession, and statistical inference. J Am Stat Assoc 1927;22:209–12.
[32] Underwood T, Paganetti H. Variable proton relative biological effectiveness: How do we move forward? Int J Radiat Oncol Biol Phys 2016;95:56–8.
[33] Tommasino F, Widesott L, Fracchiolla F, Lorentini S, Righetto R, Algranati C, et al. Clinical implementation in proton therapy of multi-field optimization by a hybrid method combining conventional PTV with robust optimization. Phys Med Biol 2020;65:045002.
[34] Peeler CR, Mirkovic D, Titt U, Blanchard P, Gunther JR, Mahajan A, et al. Clinical evidence of variable proton biological effectiveness in pediatric patients treated for ependymoma. Radiother Oncol 2016;121:395–401.
[35] Niyazi M, Niemierko A, Paganetti H, Söhn M, Schapira E, Goldberg S, et al. Volumetric and actuarial analysis of brain necrosis in proton therapy using a novel mixture cure model. Radiother Oncol 2020;142:154–61.
[36] Lühr A, von Neubeck C, Pawelke J, Seidlitz A, Peitzsch C, Bentzen SM, et al. "Radiobiology of Proton Therapy": Results of an international expert workshop. Radiother Oncol 2018;128:56–67.
[37] Freund D, Zhang R, Sanders M, Newhauser W. Predictive risk of radiation induced cerebral necrosis in pediatric brain cancer patients after VMAT versus proton therapy. Cancers 2015;7:617–30.
[38] Lambrecht M, Eekers DBP, Alapetite C, Burnet NG, Calugaru V, Coremans IEM, et al. Radiation dose constraints for organs at risk in neuro-oncology; the European Particle Therapy Network consensus. Radiother Oncol 2018;128:26–36.
[39] Kitpanit S, Lee A, Pitter KL, Fan D, Chow JCH, Neal B, et al. Temporal lobe necrosis in head and neck cancer patients after proton therapy to the skull base. Int J Part Ther 2020;6:17–28.
[40] Stock M, Gora J, Perpar A, Georg P, Lehde A, Kragl G, et al. Harmonization of proton treatment planning for head and neck cancer using pencil beam scanning: first report of the IPACS collaboration group. Acta Oncol 2019;58:1720–30.